JOURNAL OF MATERIALS SCIENCE 24 (1989) 627–632

Observations of structural defects in web-grown silicon ribbon

Y. K. KIM, R. J. DE ANGELIS
Department of Metallurgical Engineering and Materials Science, University of Kentucky, Lexington, Kentucky 40506, USA

The dislocation configuration in web-grown silicon ribbon was investigated using chemical etching techniques. The presence of dislocation loops on twin planes is observed and accounted for by self-interstitial condensation. The interstitials were either quenched in, due to the rapid cooling of the ribbon from the solidification temperature, or produced by oxide precipitation on the twin plane. Very large faulted loops of mm size were also observed.

1. Introduction

The most common structural defects in silicon flat sheets grown from the melt are dislocations, swirls and twins. Since dislocations may reduce photovoltaic efficiency, flat plate silicon material intended for solar cell fabrication should contain a minimum density of dislocations.

The dendritic web method of growing silicon ribbon produces a thin ($\sim 100\,\mu$), flat twinned crystal whose shape is defined by the crystallography of the plate and by surface tension forces, rather than by shape-defining dies. An odd number of twin planes (greater than three) parallel to the ribbon surface is considered to be necessary to ensure stable growth of silicon sheet by the web process [1, 2]. Silicon ribbons as wide as 7 cm have been grown successfully by the web process.

The main objective of this work is to characterize a portion of the defect structure present in samples of web-grown silicon ribbon employing chemical etching techniques on the plane of the ribbon surface and on planes parallel and transverse to the growth direction. Observation of the etched surfaces of the specimen were made using optical and scanning electron microscopy.

This investigation was designed to define the defect configuration along the growth direction of the ribbon, the relationships between dislocations and the twin planes and the variations in the configuration of the structure of the ribbon through the thickness.

2. Materials and experimental procedures

Web grown silicon ribbon specimens for the present investigation were produced by the Westinghouse Electric Corp. [3]. The main attributes of the web dendritic ribbon growth processes are shown in Fig. 1. Ribbon sections from two 2.5 cm wide growth runs were investigated. One ribbon was grown at a rate of 1.16 cm/min and was 0.094 mm thick; the other was grown at 1.76 cm/min and was 0.11 mm thick.

Since silicon is brittle at the room temperature and the ribbon is between 94 and 110 μ thick, extreme care

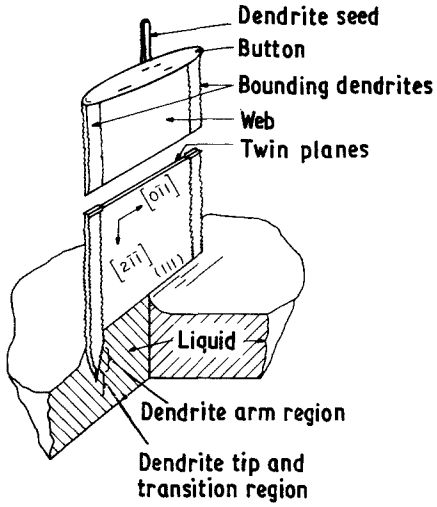

Figure 1 The web dendritic growth process and the crystallography of the ribbon.

is required in preparing specimens for metallographic observation. Samples were cut from the ribbon as-received using a diamond glass cutter. The fillet region between the edge of the web and the bounding dendrite is the thinnest part of the web and was easy to scratch and fracture. The thicker dendrite had to be heavily scratched to obtain fractures in desired positions. After scratching, covering the desired part of the silicon ribbon with adhesive tape was found to be helpful in avoiding catastrophic breakage of the whole ribbon sample when it was impacted for fracture.

The crystallographic surfaces examined were: (1 1 1), the plane of the ribbon surface; (2 $\bar{1}$ $\bar{1}$), the cross-section normal to the growth direction; and (0 1 $\bar{1}$), the cross-section parallel to the growth direction (Fig. 1). Observations of the defect configuration on these planes revealed information concerning the dislocation geometry. The polished surfaces were etched using either Sirtl solution for 1.0 to 1.5 min or Dash solution for 30 min.

In one group of experiments, the structures of the specimens were observed through the thickness by removing controlled layers of the ribbon surface using a planar etchant. After surface removal, the defects at

0022–2461/89 $03.00 + .12

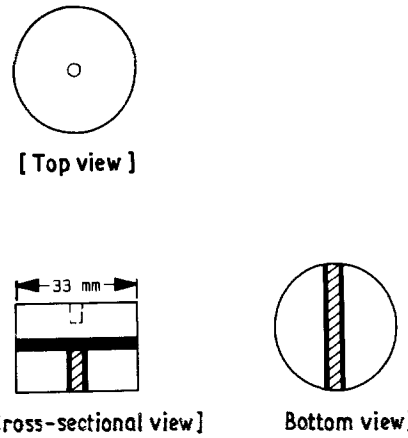

Figure 2 The metallographic mounting technique employing two waxes. (□), epoxy, (■), paraffin and (▨), silicon specimen.

that depth position were revealed by etching with Sirtl solution for 1.0 min. This procedure allowed the variation in dislocation structure approaching and at the twin planes to be observed.

Variations in oxygen content in the ribbon thickness were observed by forming oxygen-induced stacking faults employing a duplex heat treatment [4]. Heat treatment for 22 h at 700° C followed by 9 h at 1100° C in a flowing argon atmosphere was found to precipitate stacking faults ca. 4 μm long. To perform this portion of the investigation, it was necessary to remove the delicate silicon specimens from the metallographic mount, thermally treat the specimen and remount it for further observation.

The delicate silicon specimens and the requirement that the mounting material must be able to survive the preparation stages and the strong etchants, made the selection of a suitable mounting technique critical in the oxygen precipitation experiment. Low melting temperature waxes were investigated as possible mounting materials that would allow the specimen to be removed without damage. Black wax was however found to be insoluble in the strong Sirtl solution and it was difficult to separate the specimen from the black wax mount. This separation problem was solved by using paraffin wax, which was also stable in the etchants, as a mounting material. However, paraffin was found to be too soft to secure the specimen under the grinding and polishing loads required in specimen preparation and it easily smeared during polishing, coating the surface of the silicon specimen. To avoid these difficulties, a paraffin and epoxy duplex mount was developed and used successfully. The appearance of the duplex mount is shown schematically in Fig. 2. This mounting technique minimized the area of paraffin in contact with the polishing surface, reducing the smearing and coating of the specimen surface.

A special polishing procedure had to be developed to completely avoid the problem of paraffin covering on the silicon specimen surface. Initial polishing was done using a soft and thick polishing cloth that produced a convex surface on the silicon specimen and concave surface to the paraffin layer between the specimen and the epoxy. This was followed by an intermediate polish on the thinner cloth using a MINIMAT auto-polisher (distributed by Buehler Inc.). The final polishing was for 30 min using Syton 40 emulsion polishing powder. This procedure produced a specimen with a clean surface that was easily removed from the mount by melting the paraffin.

3. Results and discussion

Observations made on the etched (2 $\bar{1}$ $\bar{1}$) cross-section revealed dislocations that were mainly associated with the twin planes (Fig. 3). It is also obvious that the ribbon grown at the faster rate (Fig. 3b) contained a higher density of dislocations on the twin plane. The

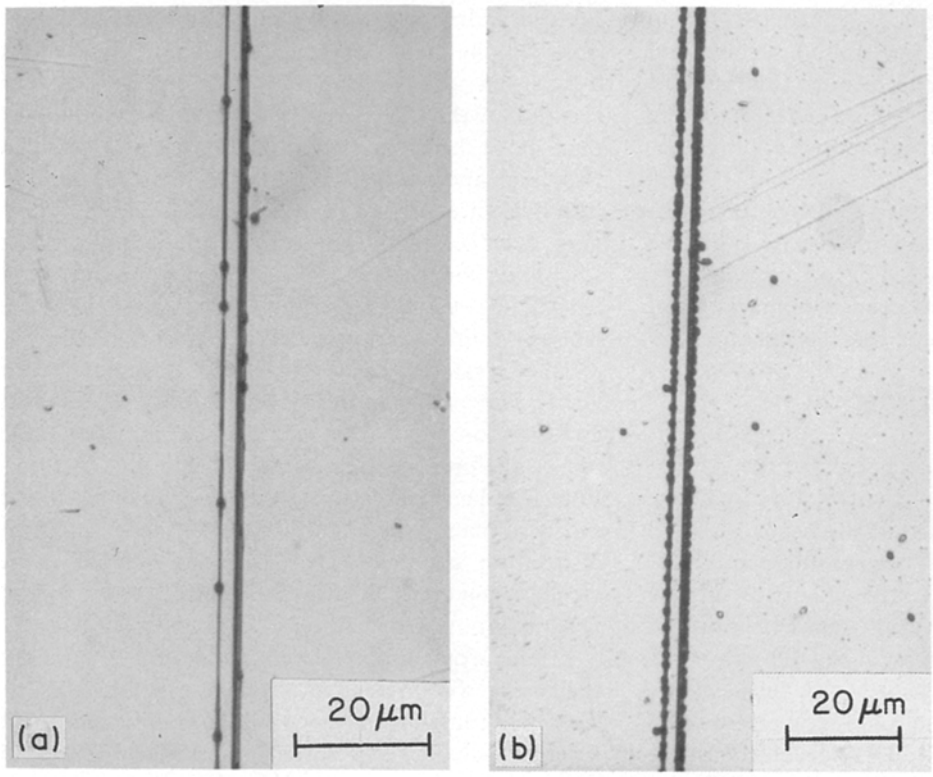

Figure 3 Optical micrograph of the (2 $\bar{1}$ $\bar{1}$) cross-section of silicon ribbons grown at: (a) 1.16 cm/min and (b) 1.76 cm/min. Sirtl solution 1.5 min.

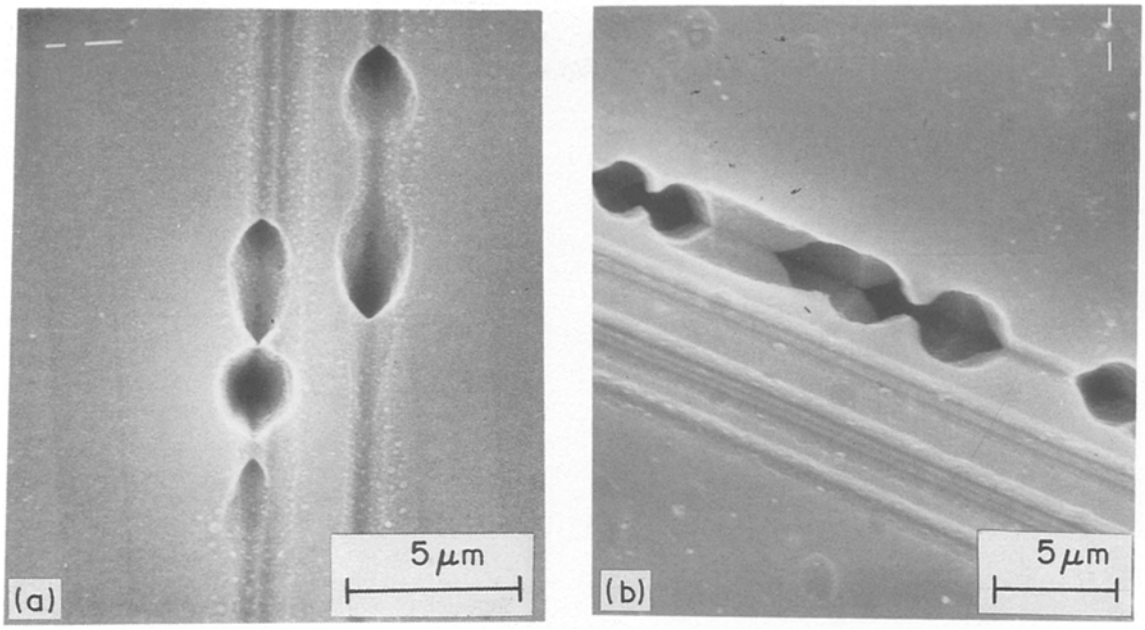

Figure 4 Scanning electron micrograph of dislocation etch pits on the $(2\bar{1}\bar{1})$ plane of silicon ribbon: (a) The geometry of the etch pits and (b) the relationship of the etch pits and the twin plane. Sirtl solution 1.5 min.

spacing of dislocations on the twin plane in the faster growth rate material is about 2 μm. In the slower-growth-rate material the dislocation spacing varies between 4 and 13 μm.

A closer observation of the dislocations made in the 1.16 cm/min. growth rate material by scanning electron microscopy (SEM) is shown in Fig. 4a. Two types of etch pit geometries are visible in this micrograph: etch pits at an angle to the surface, associated with a dislocation loop and an etch pit oriented normal to the specimen surface associated with the location of a pure edge dislocation lying parallel to the growth direction. The intimate relationship between the dislocations loops and the twin plane is shown in Fig. 4b. This micrograph shows that the etch pits actually straddle the twin plane. The dislocation loops are about 5 μm in diameter.

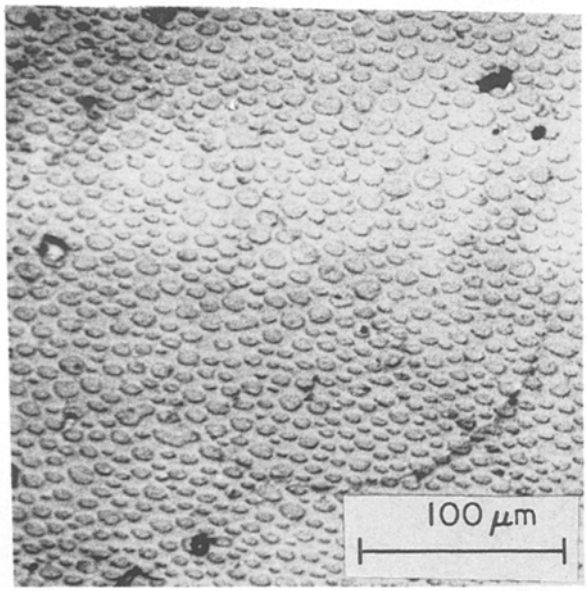

Figure 5 Optical micrograph of the (1 1 1) ribbon surfaces showing the dislocation configuration on the twin plane. Sirtl solution 1.0 min.

Controlled planar etching of the (1 1 1) surface was employed to reveal the dislocation arrangement on the twin plane. The defect structure on the twin plane was observed to consist of a high density of dislocation loops (Fig. 5). The average loop diameter is of the order of 5 μm, as was the loop size observed in Figs. 3 and 4. These loops are thought to have formed by an interstitial condensation process which indicates the twin plane is an efficient sink for point defects and has an important role in controlling the quality of web-grown silicon ribbon.

The formation of excess interstitials in the ribbon is a result of either the rapid cooling rate as the ribbon is pulled or the formation of silica particles [5] which are frequently observed on the twin planes. Precipitates of SiO_2 on the twin plane are shown in the SEM micrograph in Fig. 6. As can be seen, due to the volume increase, in the surrounding material the larger particles of SiO_2 produced sufficient strain, to develop fractures. During the formation of SiO_2, self-interstitials are emitted in a relationship of one interstitial atom for two oxygen atoms that join the oxide phase [5]. Therefore, precipitation of SiO_2 increases the concentration of interstitials on the region of the twin planes, which condense into small dislocation loops [6].

During solidification it is reasonable to expect that the oxygen content is greater in the liquid material contained in the re-entrant angles on the growth plane at the twin plane location. The geometry of the solidification front containing two twins, shown in Fig. 7, could account for the enrichment of the material in the region of the twin plane with oxygen. Figure 7 shows that the solidification front contains 141° re-entrant angles alternating with ridges having an exterior angle of 219° [1]. This interface geometry

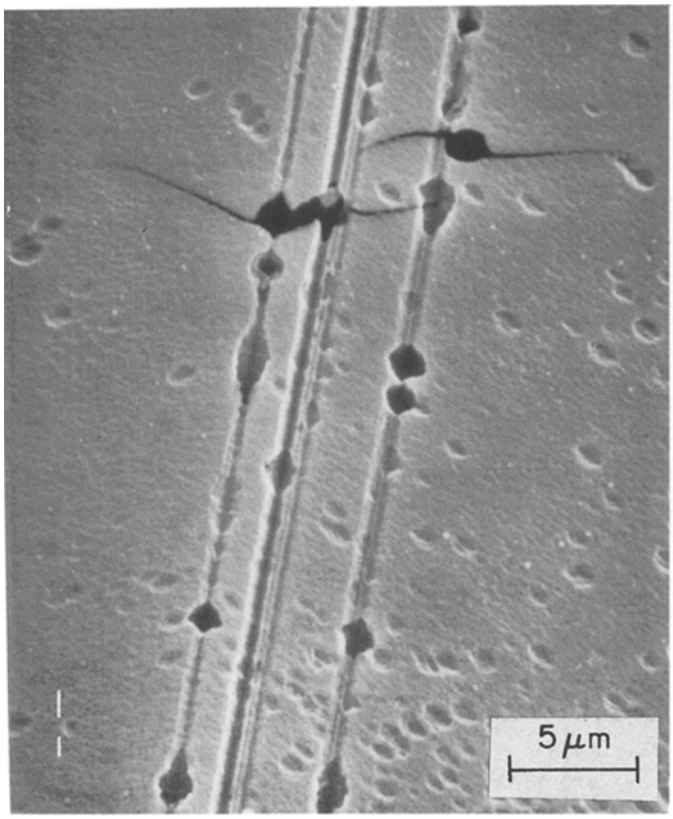

Figure 6 Scanning electron micrograph of (0 1 $\bar{1}$) plane showing oxide precipitates and the associated fracturing of the material. Sirtl solution 1.0 min.

would be expected to be associated with solute concentration variations.

A series of experiments was designed to determine the distribution of oxygen in the web. Six specimens were prepared, etched and observed optically, removed from their mounts and heat treated for 22 h at 700° C followed by 9 h at 1100° C. Typical structures observed prior to and subsequent to heat treatment are shown in Fig. 8. It is clear that a greater concentration of oxygen-related defects exists in the region of the twin plane. An oxygen deduced zone of material on either side of the twinned region contains a lower concentration of stacking faults than the material further removed from the twins. The assumption that an initial distribution of oxygen is uniform requires the oxygen, previously existing in the region near the twin planes to have diffused to the nearby twin plane. This suggests that the twin planes attract oxygen atoms. Another possibility is that all or part of this denution could have formed during solidification. It is not possible from these observations to make a definite statement concerning the mechanism of the formation of the oxygen-denuded regions adjacent to the twin planes.

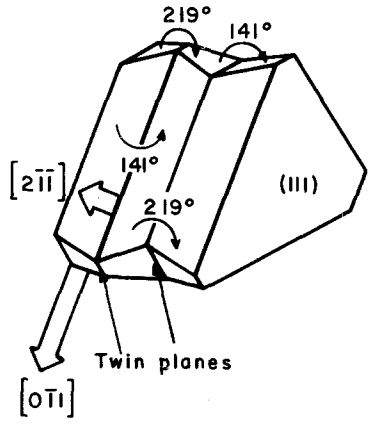

Figure 7 The crystallography of the solidification front in a crystal containing two twins.

The defect structure observed on the (0 1 $\bar{1}$) plane contained faulted loops extending 1 to 2 mm along the growth direction. Portions of two such loops are shown in the optical micrograph in Fig. 9. This observation was totally unexpected. These appear to be interstitial loops that formed near the L/S interface and continued to grow by collecting interstitial point defects present in the interface region. Notice that the side of the twin plane on which the large loops lie contains no small dislocation loops. Interstitial stacking disorders are identical in structure to a microtwin with a stacking sequence, Aa Bb Cc A/a Cc B/b Cc Aa Bb, where / denotes the location of a twin plane [7]. This defect can annihilate by forming on an existing twin plane. This process produces a two plane growth of the existing twin.

The large faulted dislocation loops are not considered to have formed by actually reaching the liquid because of the fast pulling speed of the web and because of the existence of the bounding dislocations on both sides of the fault. If these faulted dislocation loops formed by extending to the liquid–solid interface, both bounding dislocations would not be present in the ribbon because they can grow infinitely. In addition, the region of highest compressive stress is at the liquid–solid interface [8], which would also be the location of a minimum in interstitial content. This condition would tend to stop the loop from growing into the liquid.

The approximation of the radius of the faulted dislocation loops, which were assumed to grow due to the supersaturated interstitials, can be performed

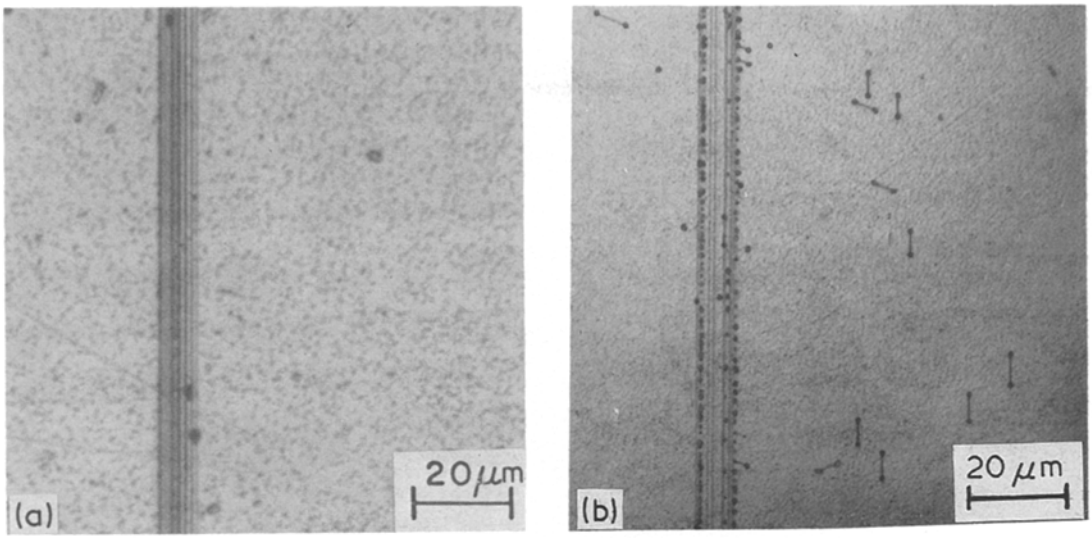

Figure 8 Optical micrograph of (2 $\bar{1}$ $\bar{1}$) plane of silicon ribbon: (a) Prior to heat treatment and (b) same specimen as in (a) after 9 h at 700° C and 9 h at 1100° C. Sirtl solution 1.5 min.

using the toroidal approximation method employed by *Wada et al.* [4] in a study of the growth kinetics of the two-dimensional stacking fault in the CZ-grown silicon crystal. Using this method, the radius of a stacking fault of 0.25 mm was calculated to be able to form at a distance 3 cm from the liquid–solid interface.

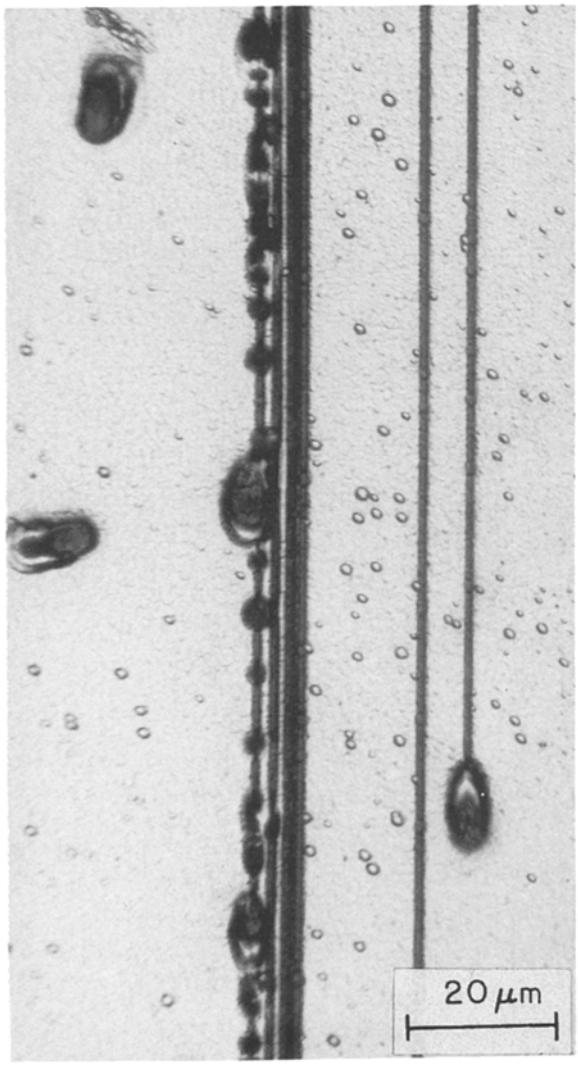

Figure 9 Optical micrograph of (0 1 $\bar{1}$) plane showing twin planes, dislocations on the twin plane and portions of two large faulted dislocation loops. Dash solution for 30 min.

The measured diameters of these faulted large dislocation loops were in the range of 0.038 to 2.3 mm. The formation of the large sized (2.3 mm) stacking faults were observed to exist only near the twin planes, again suggesting the presence of an excess concentration of interstitials formed from the silicon dioxide clusters located at the twin planes.

It is interesting to attempt to show that it is possible to account for all the interstitials required to form the dislocation loop array on the twin plane (Fig. 5). The number of interstitial atoms required per cm^2 of fault is 8.0×10^{14} atoms/cm^2 [9]. Using a measured loop density of $1.3 \times 10^6/cm^2$ and an average diameter of 5×10^{-4} cm gives 0.25 cm^2 of loop per cm^2 of ribbon. If the ribbon is 100 μm thick, then there exists 0.25 cm^2 of loop per 0.01 cm^3 of silicon. The equilibrium concentration of interstitials in this volume of material at the melting point is 2×10^{14} (interstitials/0.01 cm^3) [10]. If one half of these arrived at the twin plane, they would produce 0.12 cm^2 of fault, ca. half of the area of faulted loop observed. To account for the remaining area of fault requires 2×10^{14} interstitials, which would be produced by the precipitation of 4×10^{14} oxygen atoms into silica on 1.0 cm^2 of twin plane. The ribbon material contains 10^{18} oxygen atoms/cm^3, or 4×10^{14} atoms of oxygen in a 4 μm by 1 cm^2 region. The means that sufficient oxygen to produce the required interstitials is in a 4 μm thick region about the twin plane. The oxygen-denuded zone in Fig. 8b extends about 8 μm from the twin planes. Thus there is no difficulty in accounting for all of the interstitials required to form the dislocation loops observed on the twin planes as either being produced at the melting temperature or by the formation of oxide precipitates on the twin plane.

Acknowledgements

This research was sponsored by DOE/SERI through Contract No. XL-7-06123-1.

References

1. D. R. HAMILTON and R. G. SEIDENSTICKER, *J. App. Phys.* **31** (1960) 1165–1168.

2. E. BILLIG, *Proc. R. Soc.* **A229** (1955) 346–363.
3. R. G. SEIDENSTICKER and R. H. HOPKINS, *J. Cryst. Growth* **50** (1980) 221–235.
4. K. WADA, N. INOVE and J. OSAKA, "Precipitation of Oxygen and Mechanisms of Stacking Fault Formation in Czochralski Silicon Bulk Crystals", Defects in Semiconductors II (Elsevier, New York, 1983) pp. 125–139.
5. A. BOURRET, "Oxygen Aggregation in Silicon", Proceedings of the 13th International Conference on Defects in Semiconductors (Metallurgical Society of AIME, 1984) pp. 129–146.
6. W. PATRICK, E. HEARN and W. WESTDROP, *J. Appl. Phys.* **50** (1979) 7156–7164.
7. O. L. KRIVANEK and D. M. MAHER, *Appl. Phys. Lett.* **32** (1978) 451–453.
8. O. W. DILLON, Jr., C. T. TSAI and R. J. De ANGELIS, *J. Appl. Phys.* **60** (1986) 1784–1792.
9. B. LEROY, *ibid.* **53** (1982) 4779–4785.
10. H. FOLL, V. GOSELE and B. O. KOLBESEN, *J. Cryst. Growth* **40** (1977) 90–108.

Received 4 January
and accepted 9 May 1988